Deconvolution and Assignment of Different Optical Transitions of the Blue Copper Protein Azurin from Optically Detected Electron Paramagnetic Resonance Spectroscopy

Birgit Börger,*,† Jörg Gutschank,† Dieter Suter,† Andrew J. Thomson,‡ and Stephen J. Bingham§

Fachbereich Physik, Universität Dortmund, 44221 Dortmund, Germany, Centre for Metalloprotein Spectroscopy and Biology, School of Chemical Sciences, University of East Anglia, Norwich NR4 7TJ, U.K., and Department of Physics, University of Bath, Bath BA2 7AY, U.K

Received September 12, 2000. Revised Manuscript Received November 28, 2000

Abstract: Magnetic circular dichroism is a powerful spectroscopic tool for the assignment of optical resonance lines. An extension of this technique, microwave-modulated circular dichroism, provides additional details, in particular information about the orientation of optical transition moments. It arises from magnetization precessing around the static magnetic field, excited by a microwave field, in close analogy to electron paramagnetic resonance (EPR). In this paper we investigate the visible and *near-infrared* spectrum of the blue copper protein *Pseudomonas aeruginosa* azurin. Using a nonoriented sample (frozen solution), we apply this technique to measure the variation of the optical anisotropy with the wavelength. A comparison with the optical anisotropies of the possible ligand-field and charge-transfer transitions allows us to identify individual resonance lines in the strongly overlapping spectrum and assign them to specific electronic transitions. The technique is readily applicable to other proteins with transition metal centers.

1. Introduction

The blue copper site is found in various proteins containing a single copper center, such as azurins, plastocyanins, and stellacyanins. These systems play an important role as electron carriers in electron-transfer chains.[1,2] They owe their name to their intense blue color, arising from a strong absorption band centered at 630 nm.

Various spectroscopic techniques have been used to unravel the electronic structure of these interesting compounds. Working with a single crystal of the blue copper protein plastocyanin and using polarized absorption measurements, Solomon and coworkers showed that the dominating optical transition giving rise to the blue band is a charge-transfer Cu−Cys S transition.[3,4] Using magnetic circular dichroism spectroscopy (MCD), they could deconvolute the optical absorption spectrum and associate the individual bands with transitions to excited states calculated from a crystal field model. Electron paramagnetic resonance spectroscopy (EPR) revealed the approximately axial symmetry of the ground-state **g**-"tensor" and a characteristic hyperfine broadening due to the copper nuclear spin ($I = 3/2$). Single-crystal EPR studies of plastocyanin[5] and azurin[6] showed that the g_z-axis is almost parallel to the bond from the copper to the sulfur of a methionine ligand. This defines the *z*-axis of the site and places the half-occupied d_{xy}-orbital perpendicular to this axis approximately in a plane defined by two histidine ligands and a cysteine.[7]

In this paper we demonstrate a new spectroscopic technique that yields the polarization of optical absorption lines without requiring single crystals. We apply this technique to *Pseudomonas aeruginosa* azurin, where no single-crystal absorption measurements have been published so far. Our technique is based on coherent Raman-detected EPR,[8,9] which correlates the optical anisotropy with the EPR spectrum. This correlation of **g**-"tensor" and optical anisotropy has also been achieved by measuring MCD magnetization curves,[10,11] but in practice the latter technique is only successful if the *g*-anisotropy is significantly larger than in azurin.[12]

The alternative which we demonstrate here is to measure the microwave-modulated MCD[8] due to *transverse* magnetization precessing around the static magnetic field B_0. Like in conventional EPR, this magnetization is excited by a resonant microwave field. A circularly polarized laser beam perpendicular to the static field probes the magnetization in the direction of the laser field. The precessing spins modulate the absorptivity of the sample for circularly polarized light and the transmitted laser beam is therefore modulated at the microwave frequency.

† Universität Dortmund.
‡ University of East Anglia.
§ University of Bath.

(1) Solomon, E. I.; Lowery, M. D. *Science* **1993**, *259*, 1575.
(2) Sykes, A. G. *Adv. Inorg. Chem.* **1991**, *36*, 377.
(3) Solomon, E. I.; Hare, J. W.; Dooley, D. M.; Dawson, J. H.; Stephens, P. J.; Gray, H. B. *J. Am. Chem. Soc.* **1980**, *102*, 168.
(4) Gewirth, A. A.; Solomon, E. I. *J. Am. Chem. Soc.* **1988**, *110*, 3811.
(5) Penfield, K. W.; Gay, R. R.; Himmelwright, R. S.; Eickman, N. C.; Norris, V. A.; Freeman, H. C.; Solomon, E. I. *J. Am. Chem. Soc.* **1981**, *103*, 4382.
(6) Coremans, J. W. A.; Poluektov, O. G.; Groenen, E. J. J.; Canters, G. W.; Nar, H.; Messerschmidt, A. *J. Am. Chem. Soc.* **1994**, *116*, 3097.
(7) Solomon, E. I.; Baldwin, J. B.; Lowery, M. D. *Chem. Rev.* **1992**, *92*, 521.
(8) Bingham, S. J.; Suter, D.; Schweiger, A.; Thomson, A. J. *Chem. Phys. Lett.* **1997**, *266*, 543.
(9) Suter, D. *The Physics of Laser-Atom Interactions*; Cambridge University Press: Cambridge, U.K., 1997; Chapter 3.
(10) Thomson, A. J.; Cheesman, M. R.; George, S. J. *Methods Enzymol.* **1993**, *226*, 199.
(11) Oganesyan, V. S.; George, S. J.; Cheesman, M. R.; Thomson, A. J. *J. Chem. Phys.* **1999**, *110*, 762.
(12) Neese, F.; Solomon, E. I. *Inorg. Chem.* **1999**, *38*, 1847.

10.1021/ja003357b CCC: $20.00 © 2001 American Chemical Society
Published on Web 02/15/2001

When this modulation is measured as a function of the static magnetic field strength, one obtains optically detected EPR spectra,[8] where the different components (*C*-parameters) of the optical anisotropy contribute to different parts of the EPR spectrum. In this paper we show how this experiment allows one to measure the orientations of the electric dipole transition moments in the molecular frame. From the wavelength dependence of the optical anisotropy, we deconvolute the optical spectrum, extract the polarization of the individual transitions, and use this information to determine the electronic structure.

2. Optical Anisotropy from EPR Line Shape

To illustrate how the orientation of optical dipole moments can be determined from optically detected EPR spectra, we consider a molecule with an axially symmetric **g**-"tensor". We refer to the g_z-axis as the molecular *z*-axis, while the orthogonal components are labeled as $g_x = g_y = g_\perp$. As in conventional EPR, the magnetic resonance condition is $\hbar\omega_0 = g(\theta)\mu_B B_0$, where θ is the angle between the molecular *z*-axis and the static magnetic field B_0 and μ_B is Bohr's magneton. The orientation-dependence of the *g*-factor is $g(\theta)^2 = g_z^2 \cos^2\theta + g_\perp^2 \sin^2\theta$.[13] The laser beam propagates along the laboratory *x*-axis, perpendicular to the direction of the static magnetic field. Our experiment measures the circular dichroism originating from the fictious spin in the direction of the laser beam. In MCD, this contribution to the circular dichroism is known as the *C*-term[14] and the proportionality factor between the magnetization and the dichroism can be described with a matrix whose principal components are C_i, $i = x, y$, and *z*. These parameters may be expressed by the optical dipole operators m_j and m_k along the corresponding molecular axis:[15,16]

$$C_i = \epsilon_{ijk} Im \sum_E \langle G(i)|m_j|E\rangle\langle E|m_k|G(i)\rangle \qquad (1)$$

The sum runs over the excited states $|E\rangle$, $|G(i)\rangle$ are the relevant ground states, and ϵ_{ijk} represents the antisymmetric Levi−Civita tensor.

Since the optical and magnetic anisotropy are fixed to the same molecular axis system, the spectral position (determined by the *g*-value matrix) and the amplitude (determined by the *C*-parameter matrix) are correlated and the resulting line shape strongly deviates from a conventional EPR experiment. To illustrate this, we state that the principal *g*- and *C*-value axes coincide and first assume that C_z, which is defined to lie along the g_z-axis, is the only nonvanishing component. The main signal contribution arises then from molecules whose symmetry axis lies along the laser beam (see Figure 1b). For those molecules, the magnetic field is parallel to $g_\perp$ and the microwave excitation of the transverse magnetization is most efficient when the static magnetic field matches the resonance condition $B_0 = \hbar\omega_{mw}/(g_\perp\mu_B)$, where ω_{mw} is the microwave frequency. For molecules whose molecular *z*-axis lies along the magnetic field, the laser beam propagates in the *xy* plane, where the MCD sensitivity vanishes, and the signal at the corresponding field position is negligible (Figure 1a). For an intermediate orientation the signal amplitude is obtained by projecting the laser beam and the magnetization onto the *z*-direction, resulting in a weight factor of $\sin^2\theta$.

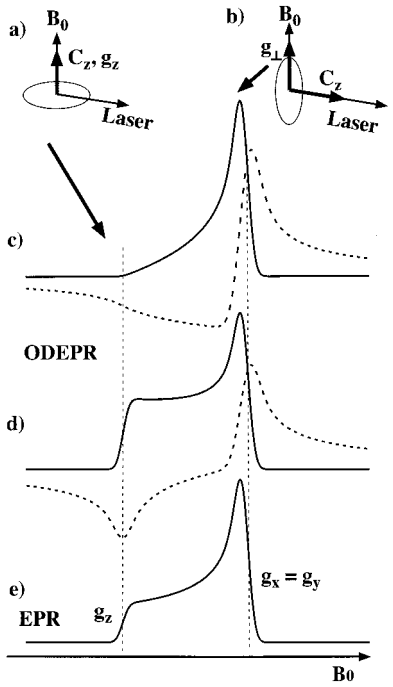

Figure 1. (a) Molecules whose *z*-axis is parallel to the magnetic field do not contribute to the signal if $C_x = C_y = 0$. The shaded disk represents the *xy*-plane of the molecule. (b) For molecules with C_z parallel to the laser beam, the EPR resonance condition is determined by $g_\perp$. (c) Calculated ODEPR absorption and dispersion spectra (solid and dashed line, respectively) of an axially symmetric species for $C_x = C_y = 0$. Note the vanishing signal at g_z. (d) Calculated ODEPR absorption and dispersion spectra (solid and dashed line, respectively) of an axially symmetric species for $C_z = 0$. The signal at $g_\perp$ decreases. (e) Calculated conventional EPR absorption spectrum of the same species. Comparison between the traces shows the orientational selectivity of ODEPR.

If in contrast the optical anisotropy is perpendicular to the *z*-axis ($C_z = 0$), the strongest signal contributions arise from molecules for which the laser beam propagates perpendicular to the symmetry axis. The total signal contribution from such molecules is proportional to $1 + \cos^2\theta$ if the effect of *g*-value anisotropy is small.

These weight factors describe the dependence of the signal on the orientation of the molecules relative to the laser beam. To calculate actual spectra, one needs to take into account also the effect of *g*-value anisotropy on the efficiency of the microwave excitation and on the evolution of the magnetization. A detailed calculation[15,16] shows that for an axially symmetric system the microwave modulated MCD $\Delta\epsilon_x$ along the direction of laser beam propagation is

$$\Delta\epsilon_x \propto T(\theta) f(\theta,\sigma)\left[C_z g_z \frac{g_\perp^2}{g^2}\sin^2\theta + C_\perp g_\perp\left(\frac{g_z^2}{g^2}\cos^2\theta + 1\right)\right] \qquad (2)$$

where $T(\theta) = \tanh(g(\theta)\mu_B B_0/2kT)$ is the Boltzmann factor, $f(\theta,\sigma)$ is a line shape function with line width σ, and $C_\perp = (C_x + C_y)/2$.

Figure 1c shows the corresponding ODEPR powder spectrum for an axially symmetric **g**-"tensor" and $C_\perp = 0$. This ODEPR spectrum shows a strong decrease in the field region of the g_z-resonance stemming from vanishing signal contribution from molecules whose symmetry axis lies along B_0. In row d the ODEPR spectrum for $C_z = 0$ is given. For comparison, the bottom row e depicts the conventional absorption EPR spectrum.

(13) Abragam, A.; Bleaney, B. *Electron Paramagnetic Resonance of Transition Ions*; Oxford University Press: Oxford, U.K.,1961; Chapter 3.
(14) Stephens, P. J. *Adv. Chem. Phys.* **1976**, *52*, 3489.
(15) Bingham, S. J.; Börger, B.; Gutschank, J.; Suter, D.; Thomson, A. J. *JBIC* **2000**, *5*, 30.
(16) Bingham, S. J.; Gutschank, J.; Börger, B.; Suter, D.; Thomson, A. J. *J. Chem. Phys.* **2000**, *113*, 4331.

3. Experimental Section

The sample consisted of a buffered aqueous solution of azurin from *Pseudomonas aeruginosa*, mixed with a glassing agent (glycerol 1:1 v/v) to obtain a glass with good optical quality at low temperatures. For the ODEPR experiment the concentration was approximately 4.6 mM, and the optical path length was 0.5 mm.

For the measurement of the coherent Raman detected EPR spectra the sample was placed in a rectangular cavity and excited by a weak microwave field with a frequency of 13.6 GHz. A variable magnetic field was provided by a superconducting split coil magnet. A laser beam parallel to the microwave field detected the precessing magnetization. We used a number of different laser sources to cover the wavelength range from 450 to 850 nm, where we expect ligand-field as well as charge-transfer transitions: an argon-ion laser for the wavelengths between 459 and 514 nm; a diode-pumped, frequency doubled Nd:YVO_4 laser with a single line at 532 nm; a ring dye-laser with Rhodamine 110 operating between 545 and 560 nm; a ring dye-laser with Rhodamine 6G between 570 and 610 nm; a Ti-saphire ring laser and a diode-laser for wavelengths in the near-infrared. The amplitude modulation of the transmitted light was detected with a high-speed photodiode (bandwidth 21 GHz, diameter of active area 25 μm). Demodulation of this microwave signal with a quadrature mixer allowed the simultaneous detection of absorption and dispersion components of the EPR signal. The polarization of the light was modulated between right and left circularly polarized by a photoelastic modulator. A more detailed discussion of the instrument is published elsewhere.[17] ODEPR spectra were measured at 1.8 K with a microwave power of 100 mW and plotted as $\Delta\epsilon_x$, the difference in extinction coefficients for left and right circularly polarized light along the direction of the laser beam. The broad band longitudinal MCD spectrum of azurin was recorded using a commercial JASCO J-500 D spectrometer.

4. Experimental Results and Analysis

4.1. Wavelength Dependence of the Optical Anisotropy. Over the wavelength range covered, the amplitude and shape of the optically detected EPR spectra show strong variations. Figure 2b−d summarizes some typical line shapes. Only the dispersion signal is shown, since the absorption signal is strongly saturated under our experimental conditions. Line shapes at all wavelengths differ from that of the conventional EPR dispersion spectrum, which is shown in Figure 2a for comparison. The experimental spectra are compared to theoretical spectra, where the ratio of $C_\perp$ to C_z was adjusted to produce the best fit to the experimental data.

To fit the experimental spectra, we first extracted the additional spectral parameters such as g-values, hyperfine coupling constant, and line width from the conventional EPR spectrum measured at 9.6 GHz. Good agreement between theoretical and experimental data was obtained with an axially symmetric model, without taking the rhombic distortion into account that is visible at higher frequencies.[6] The hyperfine coupling to the copper nucleus (single isotope, $I = 3/2$) was taken into account to first order. The best fit was obtained with the following parameters: $g_z = 2.26$; $g_\perp = 2.045$; $A_z = 172$ MHz; $A_\perp = 27$ MHz; a homogeneous line shape $f(\sigma, \theta)$ equal to a Gaussian with a line width $\sigma = 55$ MHz. These parameters are in agreement with values found in the literature.[18,19]

These parameters were used as a starting point for fitting the optically detected EPR spectra according to eq 2. An adequate simulation of most spectra at 1.8 K was possible with $\sigma = 125$ MHz. The results are shown as solid lines in Figure 2. The

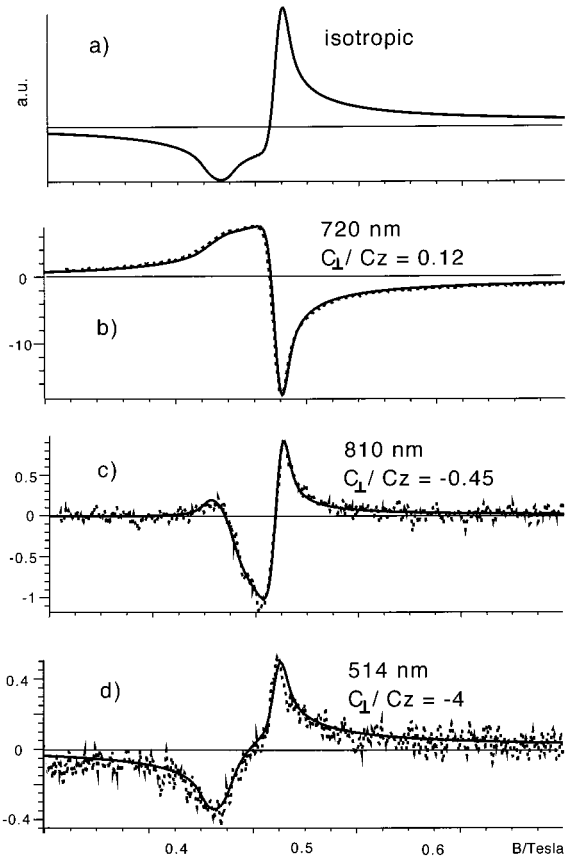

Figure 2. Dispersion type ODEPR spectra of azurin at different optical wavelengths in units of $\Delta\epsilon_x \times 10^{-3}$ M^{-1} cm^{-1} (dashed line). Fit curves were calculated according to eq 2 (solid line).

spectrum at 720 nm (13 899 cm^{-1}) is a typical example for predominantly C_z-MCD, since contributions from molecules with g_z parallel to B_0 are suppressed in the spectrum (compare Figure 1c). We calculated a ratio $C_\perp/C_z = 0.12 \pm 0.04$. The spectrum at 514 nm (19 455 cm^{-1}) shows predominantly $C_\perp$-MCD ($C_\perp/C_z = -4 \pm 2$) as can be seen from the strong emphasize of the g_z-resonance and the relatively short peak at the $g_\perp$-resonance (compare Figure 1d). Finally the spectrum at 810 nm (12346 cm^{-1}) with $C_\perp/C_z = -0.45 \pm 0.04$ is an example of a region with mixed polarizations.

The larger homogeneous line width of the ODEPR spectra compared to the conventional EPR spectra (125 MHz vs 55 MHz) may be an indication of partial saturation at 1.8 K. Temperature-dependent studies showed that around 50 K, where relaxation is faster, the line width of the ODEPR spectra decreases to values obtained from conventional EPR. The ratio of $C_\perp/C_z$ is not affected by this behavior. Light power dependent studies and microwave power dependent studies also show that the influence of the saturation on the dispersion is weak. Thus, information about optical anisotropies can be extracted even if saturation effects occur.

The relevant quantity for our analysis is the ratio of the two C-parameters, which may conveniently be expressed as an orientation angle: $C_z = C \cos\gamma$ and $C_\perp = C \sin\gamma$. Since the absolute value of $C_\perp$ and C_z cannot be extracted from the spectra, we have for convenience introduced a factor k which scales C in such a way that comparison with the longitudinal MCD bands is possible.

Figure 3 shows the variation of these parameters with the detection wavelength. The filled squares represent γ and the open squares kC. The inset defines γ. In the intermediate energy

(17) Bingham, S. J.; Börger, B.; Suter, D.; Thomson, A. *J. Rev. Sci. Instrum.* **1998**, *69*, 3403.
(18) Aqualino, A.; Brill, A. S.; Bryce, G. F.; Gerstman, B. S. *Phys. Rev. A* **1991**, *44*, 5257.
(19) Antholine, W. E.; Phillip, M. H.; McMillin, D. R. *Biophys. J.* **1993**, *64*, 267.

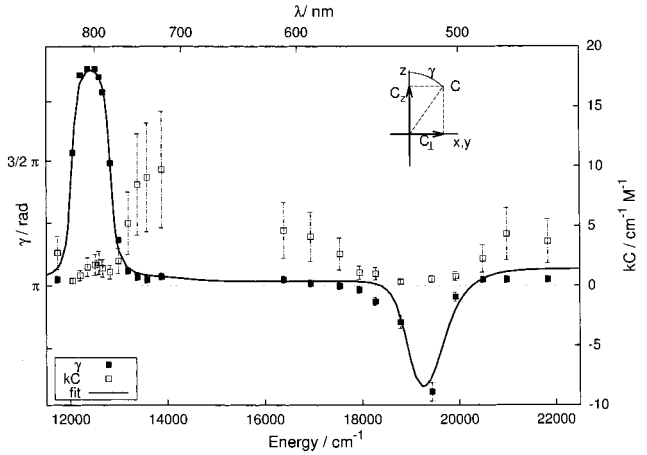

Figure 3. Fitting the ODEPR spectra gives the different C-parameters for each wavelength. The data are presented as $k\sqrt{C_z^2+C_\perp^2}$ (open squares) and $\gamma = \arctan C_\perp/C_z$ (filled squares). The fit curve for γ (solid line) was obtained with the parameters given in Table 1.

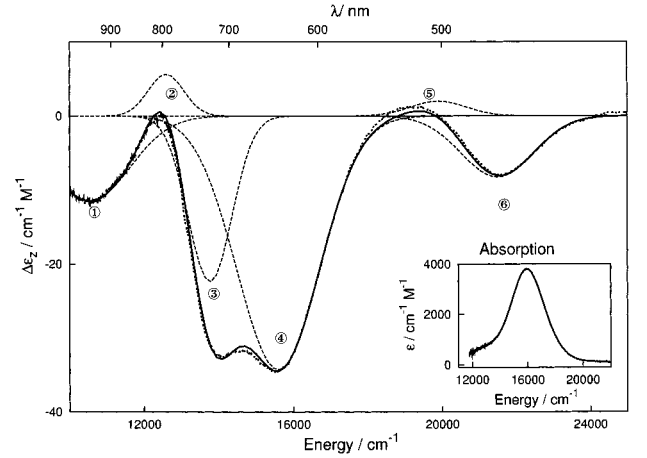

Figure 4. MCD spectrum of azurin at 1.8 K and 5 T (dotted line). Six bands, which are numbered from 1 to 6, are used to fit the features of the MCD curve in the visible region; the fit curve is given as a solid line. An inset shows the absorption of azurin.

region between 13 500 and 18 000 cm^{-1} the angle is close to π, indicating a dominating contribution of negative C_z-MCD. At 12 700 cm^{-1} γ approaches 2π, indicating that positive C_z dominates over smaller contributions of negative $C_\perp$-MCD. Around 19 200 cm^{-1} γ is close to $\pi/2$, indicating positive $C_\perp$-MCD.

In regions of high optical absorption (compare Figure 4, inset), absorption of the detection laser raised the sample temperature. This resulted in a slightly smaller line width (≈110 MHz) and a decrease of the signal size resulting from the smaller Boltzmann factor. The results obtained for the orientation angle γ are not affected by these variations, in contrast to the amplitude *kC*. Sample heating did not occur in the longitudinal MCD, which was recorded with a conventional light source at much lower intensity. As a result, the two spectra are not proportional in this wavelength range, in contrast to the usual behavior.[20] The ODEPR measurements near 19 000 cm^{-1} were obtained from a sample different from the other spectra. Differences in the optical quality of this sample led to deviations in the apparent magnitude parameter *kC* but did not affect the orientational parameter γ.

(20) Börger, B.; Bingham, S. J.; Gutschank, J.; Schweika, M. O.; Suter, D.; Thomson, A. J. *J. Chem. Phys.* **1999**, *111*, 8565.

In addition to the wavelength dependence of the ODEPR spectra, we also measured the conventional MCD spectrum, which is reproduced in Figure 4 as a dotted line. $\Delta\epsilon_z$ is the MCD given in units of the difference in extinction coefficients for left and right circularly polarized light. The exact equation for the field and temperature dependence of the MCD can be found in ref 16, eq 4. We use here a simplified form for the linear limit:[10]

$$\Delta\epsilon_z \propto g_x C_x + g_y C_y + g_z C_z = g_z C_z + 2g_\perp C_\perp \qquad (3)$$

where the second equation holds for an axial system. Due to the small *g*-value anisotropy of copper, this equation describes the relation between total MCD and *C*-terms adequately, although according to the experimental conditions (1.8 K, 5 T) we are in the strict sense not anymore in the linear limit. In contrast to ODEPR, it is for azurin practically impossible to determine both *C*-parameters with MCD spectroscopy, although for a system with a significantly larger *g*-value anisotropy temperature- and field dependent studies could be used to extract the *C*-parameters.

4.2. Band Structure. The next step in the data analysis was the decomposition into individual transitions with individual energy, line width, and optical anisotropy. The longitudinal MCD data were calculated as

$$\Delta\epsilon_z(\nu) = \sum_i \Delta\epsilon_{zi} e^{(\nu-p_i)^2/2w_i^2} \qquad (4)$$

with ν indicating the photon energy and p_i and w_i the position and width of each band. $\Delta\epsilon_{zi}$ is the averaged MCD amplitude for each band.

In the case of the transverse, microwave modulated MCD (ODEPR), the precision of the magnitude *kC* is considerably lower than that of the parameter γ. Accordingly we only fitted the orientational parameter, using

$$\gamma(\nu) = \tan^{-1}\left(\sum_i C_{\perp i} e^{(\nu-p_i)^2/2w_i^2} / \sum_i C_{zi} e^{(\nu-p_i)^2/2w_i^2}\right) \qquad (5)$$

A simultaneous fit of both experimental data sets yielded the most convincing agreement when the 450−850 nm region was decomposed into six Gaussian lines. This number agrees with that found for the MCD of poplar plastocyanin.[4] The parameters that produced this fit are summarized in Table 1. In addition, the fit was restrained by eq 3. Figure 3 compares the experimental values of γ to the result of the fitting procedure, while Figure 4 compares the experimental MCD spectrum to the calculated spectrum (solid line) and shows the contributions from the individual transitions.

The errors quoted in the table are estimated from a comparison of the results from different fitting procedures, including independent fits of MCD and γ. The largest uncertainty arises from correlations between the parameters for overlapping resonance lines, in particular bands 2 and 3 and bands 5 and 6.

The fitting procedure showed that it is essential to use both data sets. As discussed above, the longitudinal MCD does not provide orientational information, while the transverse MCD does not provide sufficiently precise magnitudes. Cancellations between bands of opposite sign make the determination of band positions from the MCD alone relatively unreliable. The orientational information from the ODEPR spectra provides here a significant improvement.

The fitted curve agrees well with the experimentally determined orientation γ, particularly in the low-energy region. The

Table 1. Parameters of the Six Gaussians (Columns 2−4) Which Were Used to Fit the Azurin MCD, Figure 4[a]

band i	p_i (cm^{-1})	$\Delta\epsilon_{zi}$ (M^{-1} cm^{-1})	w_i (cm^{-1})	kC_{zi} (M^{-1} cm^{-1})	$kC_{\perp i}$ (M^{-1} cm^{-1})	γ_i
1	10 542 ± 50	−11.5 ± 0.2	1080 ± 45	−4.2 ± 1.4	−0.4 ± 0.1	1.03π ± 0.01π
2	12 594 ± 110	5.6 ± 0.4	479 ± 55	3.5 ± 0.2	−0.6 ± 0.1	1.95π ± 0.01π
3	13 766 ± 75	−22.4 ± 1	587 ± 55	−7.7 ± 0.7	−1.2 ± 0.5	1.05π ± 0.02π
4	15 592 ± 20	−34.3 ± 0.2	1105 ± 15	−13.7 ± 2.3	−0.8 ± 0.4	1.02π ± 0.01π
5	19 907 ± 200	2.0 ± 0.2	744 ± 220	0.4 ± 0.2	0.4 ± 0.2	0.25π ± 0.11π
6	21 490 ± 200	−8.3 ± 0.3	976 ± 75	−2.6 ± 0.3	−0.6 ± 0.2	1.07π ± 0.02π

[a] The C_z- and $C_\perp$-character of the major optical transitions was obtained from fitting the parameter γ (columns 5 and 6). Column 7 contains the orientational parameter $\gamma_i = \arctan(C_{\perp i}/C_{zi})$ for each band.

first four bands have strong C_z-character. The opposite sign of C_z and $C_\perp$ for band 2 leads to the peculiar line shapes encountered in this wavelength region. Clearly, the existence of band 2 is necessary to fit the ODEPR data. ODEPR can therefore help to find optical bands even where the total MCD is small (compare Figure 4). For band 5 we find strong $C_\perp$-MCD, while band 6 is again mainly C_z-polarized. Also the major features of the high-energy region, i.e., the decrease toward $\pi/2$ in the center of band 5, are well reproduced. The remaining deviations may be attributed to the small size of the MCD in this region, which results in relatively noisy spectra and larger errors (see Figure 3). In addition, the influence of the wings of optical transitions lying at higher energies have not been taken into account.

5. Comparison with Theory and Assignment

5.1. Ligand Field Transitions. The central ion of copper proteins is a d^9 system; it is therefore sufficient to consider single electron orbitals. Since the position of the principal *g*-value axes in the molecular frame has been determined from single-crystal spectroscopy,[5] we are able not only to investigate the relative orientation of the optical and magnetic system but also to determine the electronic transition dipoles along the molecular axes.

We first consider transitions between fully occupied d-orbitals and the half-filled d_{xy}-orbital, which fall into the low energy part of our spectral region. The electronic structure of blue copper proteins has been studied by various quantum chemical techniques.[5,21−23] Here we follow the choice of Gewirth and Solomon,[4] who used D_{2d}-symmetry to predict the signs of the MCD bands of plastocyanin. The *z*-axis of our molecular coordinate system is close to the Cu−Met direction, while the *x*-axis is along the Cu−Cys direction. [Please note that we have chosen a coordinate system which corresponds to the usual axes system in D_{2d}-symmetry and thus is rotated by 45° about the *z*-axis compared to the axes system used by Solomon et al.] In this symmetry the ground-state d_{xy} (i.e. the highest orbital) transforms as B_2, $d_{x^2-y^2}$ as B_1, d_{z^2} as A_1, and d_{xz} and d_{yz} as E. The only allowed transitions are those from E to B_2 in *xy*-polarization and from A_1 to B_2 for *z*-polarized light.

To calculate the MCD, we must include the electron spin and consider the double group D'_{2d}.[24] In this group d_{xy} transforms as E″ (Γ_7), $d_{x^2-y^2}$ as E″ (Γ_7), d_{z^2} as E′ (Γ_6), and d_{xz}, d_{yz} as E′ + E″ ($\Gamma_6 + \Gamma_7$).[25,26] This assignment of the orbitals to irreducible representations is also summarized in the level diagram in Figure 5.

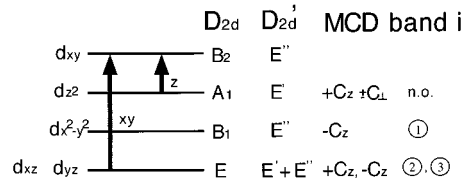

Figure 5. Level diagram of d-orbitals and states in D_{2d}-symmetry and D'_{2d}-symmetry. Allowed transitions to the half occupied d_{xy}-orbital are indicated with arrows. The polarizations of these transitions are also given. The MCD-column gives the optical anisotropies which are predicted for D'_{2d}-symmetry. The right-hand column gives the number of the assigned band allowing the comparison with Figure 4. A transition from d_{z^2} was not observed (n.o.).

We consider first the allowed transition between the B_2 (E″) ground state to the doubly degenerate state E (E′ + E″). E′ includes the $m_j = \pm 1/2$ states, and E″ the $m_j = \pm 3/2$ states. We expect negative MCD for the transition E (E″) to B_2 (E″) and positive MCD for E (E′) to B_2 (E″).[4]

The transition from B_1 is group theoretically forbidden. The transition from A_1 is allowed in *z* polarization, but the MCD should vanish. However, spin−orbit coupling mixes these states with the E-states, thus adding *xy*-character to the corresponding transitions.[27] Accordingly we expect the transition from B_1 (E″) to show negative MCD and from A_1 (E′) to show positive MCD. Considering the orientation of the MCD, we expect the *xy*-polarized transitions from B_1 and E to contribute primarily through C_z, while the transition from A_1 should contribute to C_z as well as to $C_\perp$. These predicted optical anisotropies are also given in Figure 5.

These prediction suggest the following assignment of the observed transitions (see Figure 5): band 1 (10 542 cm^{-1}) corresponds to the $d_{x^2-y^2} \rightarrow d_{xy}$ transition; band 2 (12 594 cm^{-1}) corresponds to $d_{xz} \rightarrow d_{xy}$; band 3 (13 766 cm^{-1}) corresponds to $d_{yz} \rightarrow d_{xy}$. The transition from d_{z^2} is not observed, since its transition energy is below the range observed in our experiments.[28] We have summarized the assignment of the experimentally observed bands in the right-hand column of Figure 5. Our assignment predicts the correct signs and orientations for the observed transitions and leads to the same sequence of energy levels as in plastocyanin,[4] whose active site is very similar to that of azurin.

5.2. Charge-Transfer Transitions. Transitions between d_{xy} and fully occupied ligand orbitals dominate the high-energy region of the optical spectrum. The main absorption band 4 of azurin is at 15 600 cm^{-1} (plastocyanin: 16 700 cm^{-1}). The MCD of this band is dominated by C_z (see Table 1). This can be rationalized in terms of a crystal field calculation taking into account spin−orbit coupling.[29,30] Single-crystal polarized absorption spectroscopy of plastocyanin showed that the dominant

(21) Larsson, S.; Anders, B.; Sjölin, L. *J. Chem. Phys.* **1995**, *99*, 4860.
(22) Coremans, J. W. A.; Poluektov, O. G.; Groenen, E. J. J.; Canters, G. W.; Nar, H.; Messerschmidt, A. *J. Am. Chem. Soc.* **1996**, *118*, 12141.
(23) Pierloot, K.; De Kerpel, J. O. A.; Ryde, U.; Roos, B. O. *J. Am. Chem. Soc.* **1997**, *119*, 218.
(24) Cotton, F. A. *Chemical Applications of Group Theory*; Wiley: New York, 1971; Chapter 9.
(25) Rivoal, J. C.; Briat, B. *Mol. Phys.* **1974**, *27*, 1081.
(26) Piepho, S. B.; Schatz, P. N. *Group Theory in Spectroscopy, with Applications to Magnetic Circular Dichroism*; Wiley: New York, 1983.
(27) Ballhausen, C. J. *Introduction to Ligand Field Theory*; MacGraw-Hill: New York, 1962; Chapter 6.
(28) LaCroix, L. B.; Randall, D. W.; Nersissian, A. M.; Hoitink, C. W. G.; Canters, G. W.; Valentine, J. S.; Solomon, E. I. *J. Am. Chem. Soc.* **1998**, *120*, 9621.

linear transition in this wavelength range originates from a Cys S $\pi \rightarrow$ Cu d_{xy} transition. Spin−orbit coupling mixes $d_{x^2-y^2}$-character into the ground state. As we have shown elsewhere,[15] the combination of the two transition dipoles, which are both in the *xy*-plane, leads to almost pure C_z MCD.

The remaining bands are the very weak, positive band 5 centered at 19 900 cm^{-1} with predominantly $C_\perp$-MCD and the stronger negative band 6 at 21 500 cm^{-1} with C_z character. Using the same arguments as for the Cys S $\pi \rightarrow$ Cu d_{xy} transition, we expect the transition His N → Cu d_{xy} to contribute mainly to C_z-MCD. This would allow us to assign this transition with band 6, in analogy to plastocyanin.[4] Since the **g**-"tensor" is axially symmetric, we cannot orient the dipole moment in the *xy*-plane and are therefore unable to distinguish contributions from the two histidines.

As we discussed in the previous section, the weak band 5 shows a significant $C_\perp$-MCD; i.e., this transition has components along the *z*-axis. Since this band is relatively weak, the precision of the orientation angle is relatively low for this band and does not allow a detailed analysis. However, the strong change of γ in this wavelength region shows that this weak band cannot be neglected in a theoretical treatment.[31] Gewirth et al.[4] assigns the corresponding band in plastocyanin to a Cu $d_{xy} \rightarrow$ pseudo-σ S transition. Our results are compatible with such an assignment but indicate that the transition moment is significantly tilted from the Cu−S axis.

6. Discussion

We have shown that the microwave-modulated MCD from optically detected EPR spectra provides an excellent opportunity to determine the orientation of optical transition dipoles relative to the molecular axis system. This is achieved by correlating the optical anisotropy with the known orientation of the magnetic axis system. As a result, the technique does not require single crystals but can be used on nonoriented samples such as frozen solutions.

As an example we investigated the blue copper protein azurin, of which, to the best of our knowledge, the polarizations of the optical transitions had not been measured previously. Compared to alternative methods such as MCD saturation curves, the accuracy is much higher, since different components of the optical anisotropy contribute to different parts of the ODEPR spectrum. This is particularly important in systems with small *g*-value anisotropy like copper proteins.[12]

To extract the spectral information we analyzed the active center in terms of the D_{2d}-symmetry group. While this is a relatively crude approximation of the site, it appears to lead to a consistent assignment of the optical spectrum. The molecular geometry and the high-field EPR spectra[6] indicate significant rhombic distortions from an axial symmetry, as in plastocyanin.[4] This provides an explanation for the weak but significant $C_\perp$-character in all d−d bands. For plastocyanin, Gewirth et al. have verified and refined their assignment with SCF-calculations. The similarity of these results compared with our findings shows the character of azurin as a prototypical example of blue copper proteins.

The application of this technique to azurin has clearly shown that the combination of longitudinal and transverse MCD spectra provides additional information for the distinction and assignment of optical transitions. While the absorption spectrum is almost featureless, the MCD indicates the presence of several bands. Extracting positions, amplitudes, and line widths from the MCD spectrum alone remains difficult, however, particularly in regions where bands of opposite sign overlap. The additional information on the orientation of the optical anisotropy from the transverse MCD provides significant improvement in these spectral regions. Sample heating and microwave saturation are critical points in our experiment and put limits on the accuracy of the data. We hope to overcome these problems by improving the optical quality of our samples and the construction of a 35 GHz-ODEPR spectrometer, which should provide higher resolution and make microwave saturation less likely.

Acknowledgment. We thank Dr. Vasily Oganesyan and Dr. Manfred Fiebig for helpful discussions. We gratefully acknowledge the support by the DFG through the Graduiertenkolleg Festkörperspektroskopie and the Project no. SU 192/9-1 and the UK/BBSRC through the Centre of Metalloprotein Spectroscopy and Biology.

Note Added in Proof. A recently discovered calibration problem and uncertainty in published literature data for the molar extinction coefficients for azurins (630 nm) puts a significant uncertainty on the determination of the concentration of the MCD sample and therefore the MCD amplitude in Figure 4. A scaling with a factor of approximately 4 may be necessary for column 3, 5, and 6 of Table 1. Please note that this amplitude uncertainty does not effect any conclusions drawn in the paper, which are based on the orientation angle γ rather than the magnitude.

JA003357B

(29) Abragam, A.; Bleaney, B. *Electron Paramagnetic Resonance of Transition Ions*; Oxford University Press: Oxford, U.K., 1961; Chapter 7.
(30) Pilbrow, J. R. *Transition Ion Electron Paramagnetic Resonance*; Oxford University Press: Oxford, U.K., 1990.
(31) Pierloot, K.; De Kerpel, J. O. A.; Ryde, U.; Olsson, M. H. M.; Roos, B. O. *J. Am. Chem. Soc*. **1998**, *120*, 13156.